

Complexation Behaviour of Chiral Tetradentate Polypyridines Derived from α -Pinene

Mathias Düggeli, Christophe Bonte, Alexander von Zelewsky*

Department of Chemistry, University of Fribourg, Pérolles, 1700 Fribourg, Switzerland.

Fax: +41- 26-300 97 38; Tel: +41-26-300 87 32; E-mail:

alexander.vonzelewsky@unifr.ch

A series of ligands, where two pinene-bipyridine moieties are either connected directly, or through a *p*-xylene bridge are investigated with respect to their complexation behaviour in solution. The bridged [5,6]-CHIRAGEN[*p*-xyl] ligands, which are substituted in 5' or 6' positions show self-assembly reactions, which lead to similar supramolecular species as the unsubstituted bis-pinene-bipyridines ligands studied before. The directly connected [5,6]-CHIRAGEN[0] derivatives, which are substituted at positions 5' or 6', form mononuclear complexes with helical chirality at the metal centre.

Introduction

Since the introduction of the term helicate in 1987 by Jean-Marie Lehn¹ (only a few double- and triple-stranded helicates were known before this date),²⁻⁸ the research in this field has intensified and the number of publications has been increasing rapidly (Piguet,⁹ Albrecht¹⁰). Whereas many different types of linear helicates varying the metal cations and the ligands are known,^{9,10} the knowledge about circular helicates is still very limited. Only a few circular helicates have been reported up to now¹¹⁻²² and only some of them are formed in a stereoselective fashion.¹⁸⁻²² The starting point of the present work was the hexanuclear circular helicate (Fig 1) obtained by self-assembly of the ligand ([5,6]-CHIRAGEN[*p*-xyl] **2a**, R¹ = R² = H) with copper(I) and silver(I)-cations (scheme 1).^{18,22} Our interest has focussed on the further development of this ligand by introducing new substituents R¹ and R² and on the influence of these substituents on the stereoselectivity. The key precursors for the synthesis of these CHIRAGEN derivatives **2b-d** are the

corresponding {R}-[5,6]-pinene-bipyridines **1b-d** (scheme 1).²³ From them [5,6]-CHIRAGEN derivatives with different bridges are available in one step.²⁴⁻²⁶ Whereas ligands with a *p*-xylyl-bridge **2a-d** show an interesting behaviour in the formation of self-assembled supramolecular structures^{18,22}, two directly linked pinene-bpy moieties (forming [5,6]-CHIRAGEN[0] derivatives **3a, b, d**) are designed for the formation of mononuclear complexes with a well defined stereochemistry at the metal centre (scheme 1).²⁷

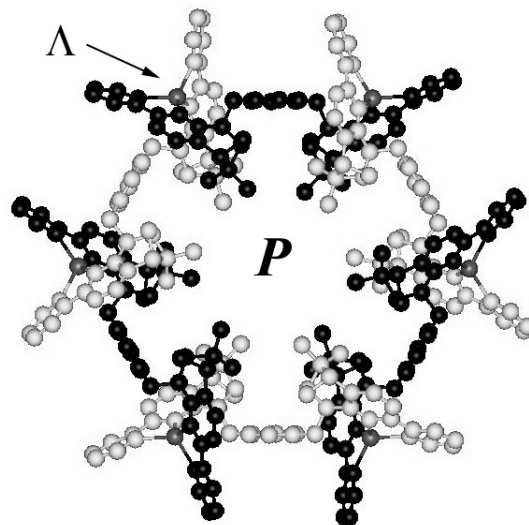
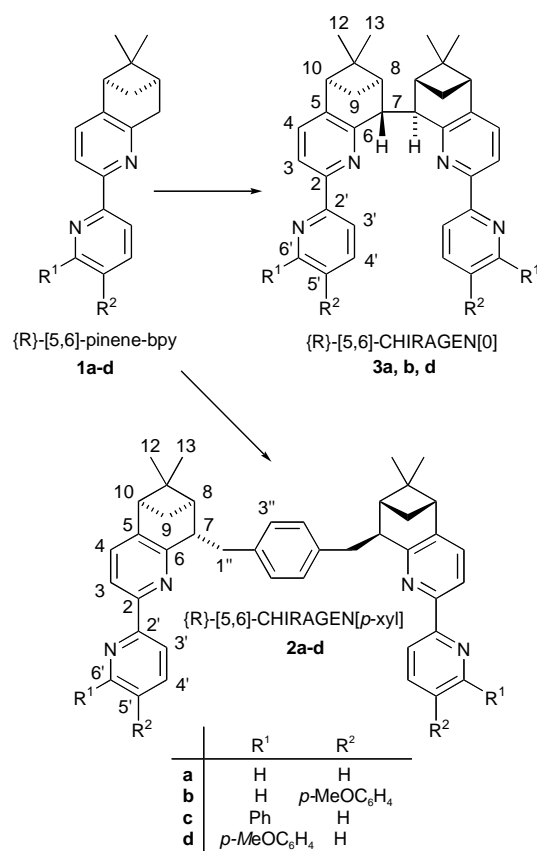


Fig. 1: X-ray-structure of the hexanuclear, circular helicate with silver(I) and ligand **2a**.¹⁸



Scheme 1: {R}-[5,6]-pinene-bpy and the corresponding tetradentate {R}-[5,6]-CHIRAGEN[bridge] derivatives.

Results and discussion

Complexes with CHIRAGEN[*p*-xyl]-derivatives

It is known, that the [5,6]-CHIRAGEN[*p*-xyl] (**2a**) forms a hexanuclear circular helicate with labile metals such as silver(I) (**4a**) and copper(I) (**5a**) (Fig 1),²² where the configuration of the ligand predetermines the configuration at the six homochiral metal centres and furthermore the configuration of the circular helicate.

The enantiopure ligand **2a** leads to a Λ -configuration at the metal centres and therefore to a P-helicate (self-recognition by self-assembly), as shown by an x-ray analysis (Fig 1).

Herein we present similar hexanuclear circular helicites with the [5,6]-CHIRAGEN[*p*-xyl] derivatives (**2b-d**) using silver(I) or copper(I). A silver(I) complex **4b** was obtained

by reaction of the ligand **2b** (dissolved in $\text{CHCl}_3/\text{CH}_3\text{CN}$) with an equimolar amount of AgPF_6 salt (dissolved in CH_3CN). The analogous copper(I)-complex **5b** was obtained in the same manner using $[\text{Cu}(\text{CH}_3\text{CN})_4]\text{PF}_6$ ²⁸ as metal cation source (yield: 99%). By addition of the ligand (dissolved in $\text{CHCl}_3/\text{CH}_3\text{CN}$) to the copper(I)-solution in CH_3CN , a red colour, the characteristic colour for a copper(I) complex with two bpy ligands, appeared immediately.

The formation of the copper(I)-complexes **5c** and **5d** of ligands **2c** and **2d**, respectively were synthesised in an analogous manner as described above. The metal source was in case of **5c** $[\text{Cu}(\text{CH}_3\text{CN})_4]\text{ClO}_4$,²⁹ in case of **5d** the $[\text{Cu}(\text{CH}_3\text{CN})_4]\text{PF}_6$ -salt.²⁸ The complexes were isolated by precipitation with diethylether to remove traces of free ligand and they showed again the characteristic red colour.

Characterization of the silver(I)-complex **4b** in solution

The ^1H -NMR-spectrum of the silver(I)-complex **4b** shows a symmetrical species (Fig 2b). As it is the case for ligand **2a**, **2b-d** cannot form mononuclear species due to sterical constraints.

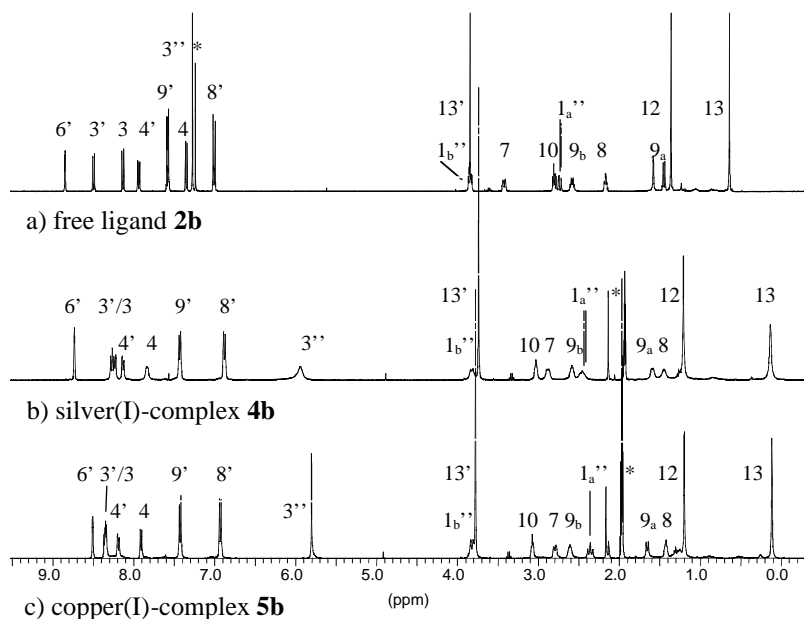


Fig. 2: ^1H -NMR-spectra of the free ligand **2b** (a) in CDCl_3 and its silver(I)-complexes **4b** (b) and its copper(I)-complex **5b** (c) in CD_3CN

Thus, the polynuclear complex is highly symmetrical, all ligands wrapping around the metal centres are equivalent. The C_2 -symmetry of the free ligand (Fig 2a) is preserved in the complex.

The largest shift of the signals upon complexation occurs for proton 3'' located on the aromatic bridge. The signals of the protons on the bridge and that of the aliphatic ones are broad at 25° C, indicating a fast exchange between two or more different species.

The comparison of the chemical shifts of signals of the complexes **4a**^{22, 30} (Fig 1) and **4b** shows only slight changes, indicating similar structures for both complexes (table 1). The protons 6' ($\Delta\delta=0.30$) and 4' ($\Delta\delta=0.16$) show the largest difference in chemicals shifts, which is caused by the influence of the methoxy-phenyl group attached at carbon 5'.

Table 1: comparison of the chemical shifts of **4a**^{22,30} and **4b**.

| | 6' | 5' | 4' | 3' | 3 | 4 | 3'' | 7 | 8 | 9a | 9b | 10 | 12 | 13 | 1a'' | 1b'' |
|----------------------------------|------|------|------|-------|------|------|------|------|-------|------|------|-------|------|------|------|------|
| 4a ^{22,30} | 8.44 | 7.43 | 7.98 | 8.27 | 8.21 | 7.83 | 5.89 | 2.82 | 1.39 | 1.57 | 2.55 | 3.01 | 1.17 | 0.08 | 2.41 | 3.73 |
| 4b | 8.74 | --- | 8.14 | 8.24 | 8.29 | 7.85 | 5.95 | 2.89 | 1.22 | 1.60 | 2.59 | 2.97 | 1.22 | 0.14 | 2.46 | 3.83 |
| $\Delta\delta$ | 0.30 | --- | 0.16 | -0.03 | 0.08 | 0.02 | 0.06 | 0.07 | -0.17 | 0.03 | 0.04 | -0.04 | 0.05 | 0.06 | 0.05 | 0.10 |

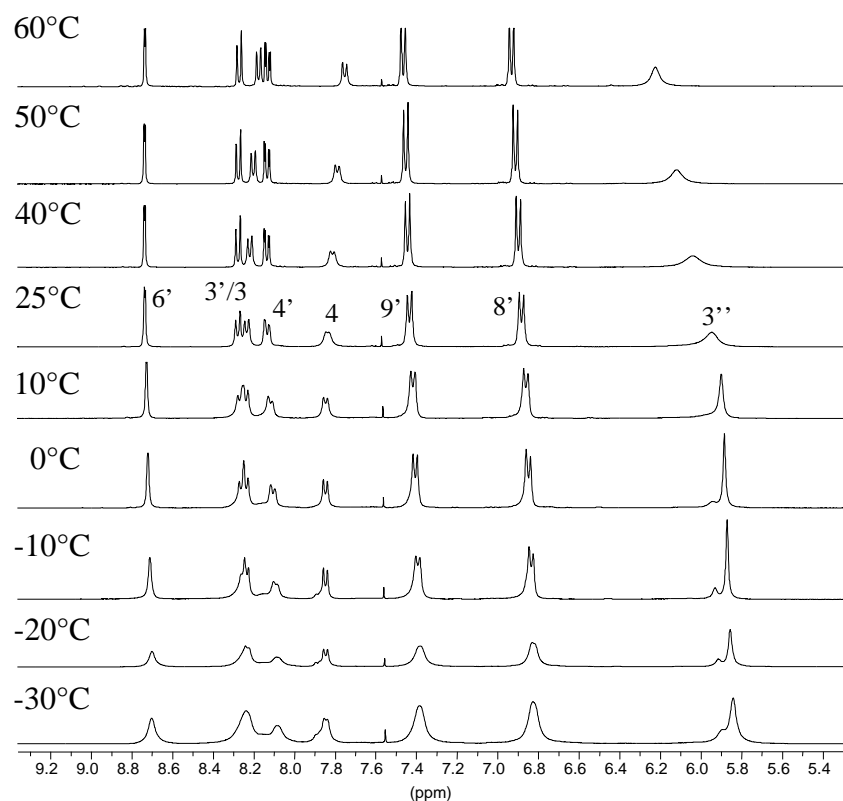


Fig. 3: Temperature dependence of ^1H -NMR-spectra of **4b** (aromatic part) in acetonitrile.

The broadening of the signals in ^1H -NMR-spectrum had been also observed in **4a**, where the hexanuclear species is in equilibrium with a tetranuclear one depending on concentration, temperature and pressure.²² ^1H -NMR-measurements of **4b** were carried out at different temperatures (Fig 3). At 60 °C all signals sharpened, the hexanuclear form is favoured at higher temperature. At lower temperatures (0 to - 40 °C) a doubling of the signals attributed to the protons at the bridge concomitant with a broadening of all signals is observed. The exchange between the two species slows down and the signals of the second species become observable (at least for the signals of the protons 3''). A doubling of all signals (Fig 4) occurs on changing the solvent. The non-coordinating solvent nitromethane inhibits the fast exchange of the two species.

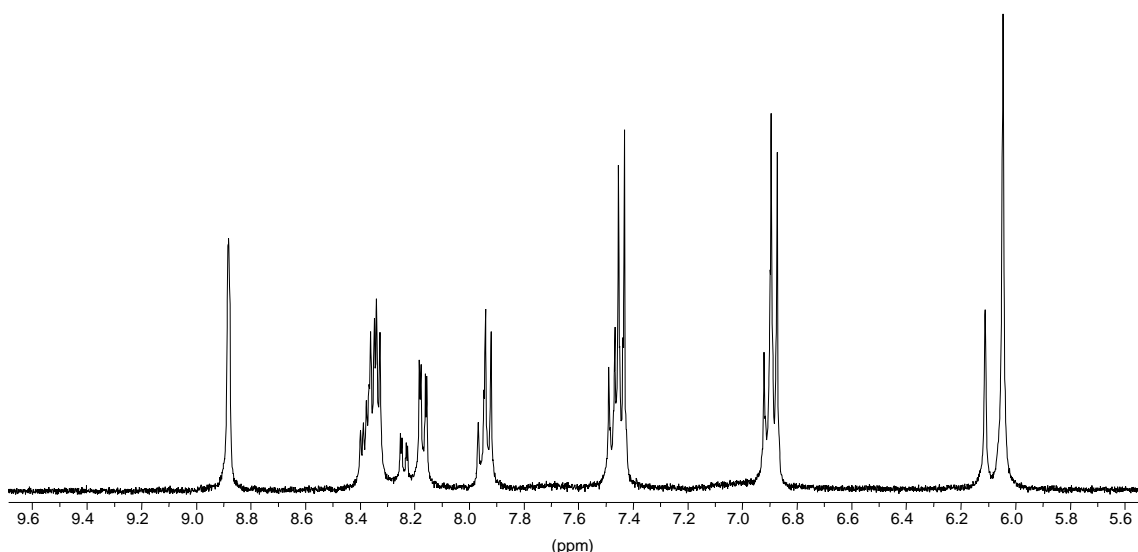


Fig. 4: Aromatic part of the ^1H -NMR of **4b** in nitromethane, 25 °C.

Electrospray mass spectroscopy is the method of choice for the analysis of such helicates, which are kinetically labile species. With this technique species in solution can be identified. In complex **4a** (structurally analysed in the solid state as hexanuclear circular helicate), electrospray mass spectroscopy shows several species present in solution.³⁰ $[\text{Ag}_6\mathbf{2a}_6](\text{PF}_6)_3^{3+}$, $[\text{Ag}_4\mathbf{2a}_4]\text{PF}_6^{2+}$ and $[\text{Ag}_2\mathbf{2a}_2]^+$ appear all at the same nominal mass (1566.5), showing, however, different isotopic pattern. The same is observed for $[\text{Ag}_6\mathbf{2a}_6](\text{PF}_6)_2^{4+}$ and $[\text{Ag}_3\mathbf{2a}_3]\text{PF}_6^{2+}$ at a mass of 1138.6. Other signals are due to $[\text{Ag}_6\mathbf{2a}_6]\text{PF}_6^{5+}$ (881.9), $[\text{Ag}_5\mathbf{2a}_5]\text{PF}_6^{4+}$ (924.7), $[\text{Ag}_5\mathbf{2a}_5](\text{PF}_6)_2^{3+}$ (1281.2) and $[\text{Ag}_4\mathbf{2a}_4]\text{PF}_6^{3+}$ (995.6). Always present are as well the peak $\text{Ag}\mathbf{2a}^+$ at 711.2 (the isotopic pattern corresponds to several species $[\text{Ag}_n\mathbf{2a}_n]^{n+}$) and $\text{Ag}\mathbf{2a}_2^+$ at 1313.9.

In the case of **4b** only a few peaks could be observed. $\text{Ag}\mathbf{2b}^+$ ($[\text{Ag}_n\mathbf{2b}_n]^{n+}$ at 922.5) and $\text{Ag}\mathbf{2b}_2^+$ (at 1737.5) have high intensities. Two other peaks correspond to the hexanuclear species. The study of the isotopic pattern of the peak at 1457.95 shows an overlapping of two species, one corresponds to the hexamer ($[\text{Ag}_6\mathbf{2b}_6](\text{PF}_6)_2^{4+}$), the other one to the trimer ($[\text{Ag}_3\mathbf{2b}_3]\text{PF}_6^{2+}$).

The NMR and ESI-MS measurements are complementary, since the formation of the circular helicates is strongly dependent on the concentration. While the NMR-technique is applicable for concentration in the range 0.01M to 0.1M, the maximum concentration for ESI-MS is around 10^{-3}M . The species observed in the ESI-MS are more abundant at

low concentration, but they are only minor species or not even observed in the NMR.

Characterization of the copper(I)-complexes **5b-d** in solution

The copper(I)-complexes (**5b-d**) of the ligands **2b-d** show similar behaviour in solution, as that observed for their analogue **5a**.³⁰

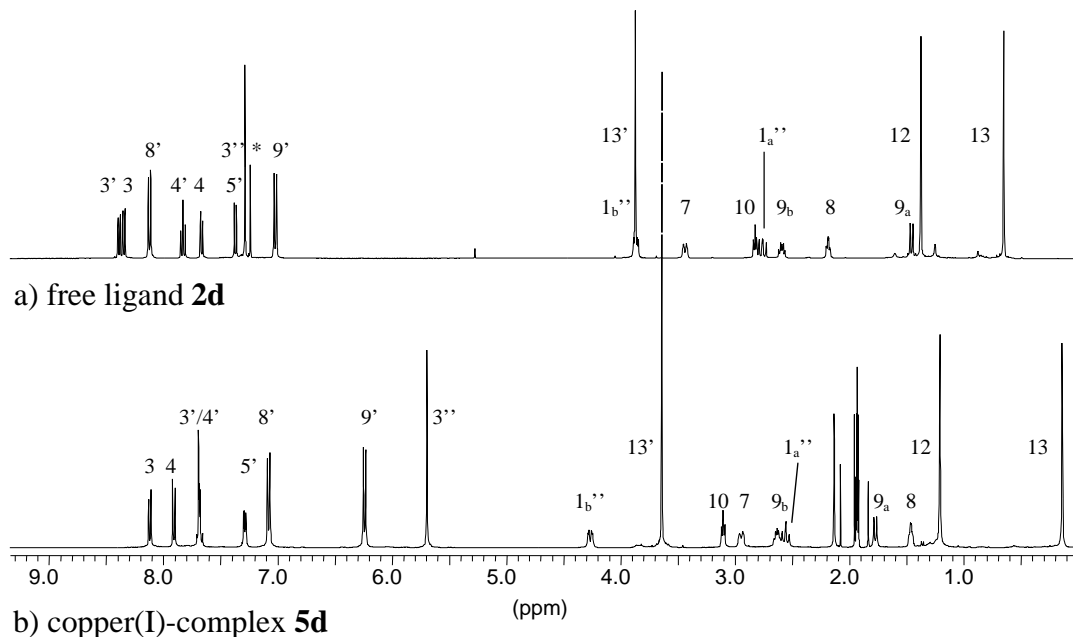


Fig. 5: ^1H -NMR-spectra of the ligand **2d** and its copper(I)-complex **5d**.

The ^1H -NMR spectra of these complexes indicate highly symmetrical, polynuclear species (mononuclear ones are excluded by the geometry of the ligands). All copper(I)-complexes show sharp signals in the ^1H -NMR-spectra in contrast to those of the silver(I)-complexes (**5b** in fig 2c, **5d** in fig 5b). Otherwise the spectra show similar characteristics as compared to its silver(I)-analogue. The signals of the protons at the bridge are sharp and show again a large upfield shift ($\Delta\delta = 1.50$ ppm for **5b**, $\Delta\delta = 1.69$ ppm for **5c** and $\Delta\delta = 1.60$ ppm for **5d**). Protons 7 and 8 are shifted significantly to high field.

The spectra of **5c** and **5d** show an additional phenomenon. The signals of the protons of the 6'-substituents are strongly shifted highfield ($\Delta\delta = 1.04$ ppm for 8', $\Delta\delta = 0.78$ ppm for 9' in both ligands and $\Delta\delta = 0.38$ ppm for 10', fig 5). All proton signals of **5b** are shifted

by nearly the same amount as compared to its analogue **5a**. The largest differences occur again for the signals of protons 6' and 4', induced by the methoxy-phenyl group at 5' (table 2). The comparison of **5a** with the complexes **5c** and **5d** shows remarkable differences in the chemical shifts (table 2), especially for the protons 3', 4', 3, 7 and both 1''. An explanation for this could be the slightly different geometries of the ligands. The 6'-substituents (themselves shifted to high field) are pointing towards the metal centre. Therewith they influence strongly the second ligand coordinated to the same centre.

The electrospray mass spectrum of **5a** does not show a peak corresponding to the hexanuclear species, which is in contrast with the X-ray analysis.¹⁸ Only peaks of the penta- ($[\text{Cu}_5\mathbf{2a}_5]\text{PF}_6^{4+}$ at 869.4 and $[\text{Cu}_5\mathbf{2a}_5](\text{PF}_6)_2^{3+}$ at 1207.4), tetra- ($[\text{Cu}_4\mathbf{2a}_4]\text{PF}_6^{3+}$ at 936.6) and trinuclear ($[\text{Cu}_3\mathbf{2a}_3]\text{PF}_6^{2+}$ at 1071.8) species could be observed. Peaks corresponding to $\text{Cu}_2\mathbf{a}^+$ ($[\text{Cu}_n\mathbf{2a}_n]^{n+}$ at 666.5) and $[\text{Cu}_2\mathbf{a}_2]^+$ (at 1270.6.5) are also present. These results are in accordance with the concentration dependence observed for the silver(I)-complexes. At low concentration several species with different nuclearities, but mostly with the ligand/metal ratio of 1:1 are in equilibrium.

Table 2 comparison of the chemical shifts of **5a**³⁰ and **5b-d**.

| | 6' | 5' | 4' | 3' | 3 | 4 | 3'' | 7 | 8 | 9a | 9b | 10 | 12 | 13 | 1a'' | 1b'' |
|-------------------------|------|-------|-------|-------|-------|-------|------|------|------|------|------|------|------|------|------|------|
| 5a ³⁰ | 8.17 | 7.40 | 7.98 | 8.31 | 5.70 | 8.3 | 7.87 | 2.69 | 1.33 | 1.59 | 2.54 | 3.02 | 1.12 | 0.02 | 2.27 | 3.68 |
| 5b | 8.48 | --- | 8.16 | 8.33 | 5.78 | 8.32 | 7.88 | 2.77 | 1.40 | 1.63 | 2.58 | 3.05 | 1.17 | 0.09 | 2.33 | 3.80 |
| Δδ | 0.31 | --- | 0.18 | 0.02 | 0.08 | 0.02 | 0.01 | 0.08 | 0.07 | 0.04 | 0.04 | 0.03 | 0.05 | 0.07 | 0.06 | 0.12 |
| 5c | --- | 7.35 | 7.71 | 7.71 | 5.69 | 8.1 | 7.91 | 2.92 | 1.45 | 1.75 | 2.63 | 3.12 | 1.21 | 0.14 | 2.57 | 4.26 |
| Δδ | --- | -0.05 | -0.27 | -0.60 | -0.01 | -0.20 | 0.04 | 0.23 | 0.12 | 0.16 | 0.09 | 0.10 | 0.09 | 0.12 | 0.30 | 0.58 |
| 5d | --- | 7.28 | 7.68 | 7.68 | 5.69 | 8.12 | 7.9 | 2.93 | 1.45 | 1.77 | 2.64 | 3.1 | 1.12 | 0.14 | 2.56 | 4.26 |
| Δδ | --- | -0.12 | -0.30 | -0.63 | -0.01 | -0.18 | 0.03 | 0.24 | 0.12 | 0.18 | 0.1 | 0.08 | 0.00 | 0.12 | 0.29 | 0.58 |

A similar behaviour was observed for the complexes **5b**, **5c** and **5d**. In each case, the major peak $[\text{CuL}]^+$ (the isotopic pattern show again the superposition of several charged species $[\text{Cu}_n\text{L}_n]^{n+}$) and the peaks corresponding to $[\text{CuL}_2]^+$ and $[\text{Cu}_2\text{L}]^{2+}$ are present. The pentanuclear species can be observed in each case, whereas peaks of the tetranuclear complex in **5b** and the trinuclear complex in **5b** and **5c** are present. The ESI-mass spectra were recorded at various concentrations (not determined), which could explain the absence of some peaks in several spectra. But it is apparent, that at low concentration several species are in equilibrium.

With the knowledge, that several species are in equilibrium at low concentration, the

UV/Vis and CD-spectroscopy should be interpreted with caution. Several species can be in equilibrium at the concentration used for UV/Vis and CD-spectroscopy. The UV/Vis spectra are similar (ϵ_{\max} at similar λ) to those of the free ligands.¹⁸

From the CD-spectra, the configuration at the metal centres can be assigned. The bands around 345 nm for **4b** and **5b**, around 306 nm for **5c** and around 317 nm for **5d** are in the positive range. The exciton coupling theory predicts for this effect an absolute configuration Λ , which is in line with the configuration found in the crystal structure of **5a**.¹⁸

Complexes with CHIRAGEN[0]-derivatives

The [5,6]-CHIRAGEN[0] is designed for the formation of mononuclear complexes, as metal cations can fit into the pocket, which is defined by the two pinene-bpy units. Complexes **6b** and **6d** are synthesised by adding a solution of AgPF_6 in acetonitrile to an equimolar solution of the ligands **3b** and **3d** in mixtures of chloroform and acetonitrile. After stirring the solution for several minutes, the solvent was removed and the solid obtained in a nearly quantitative yield.

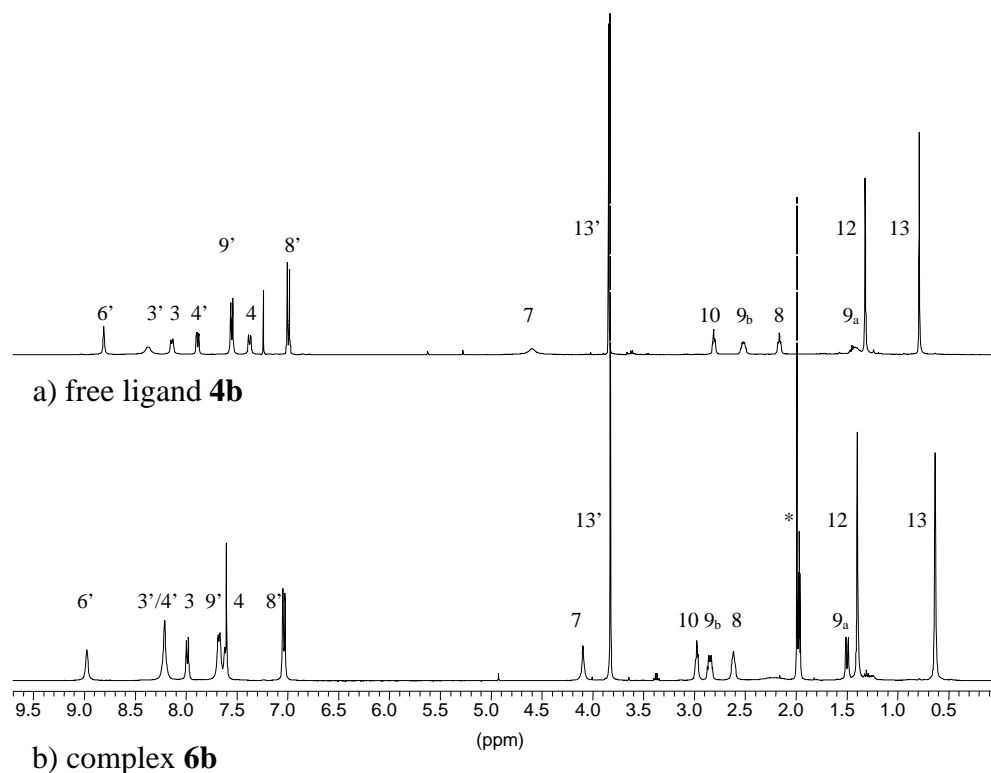


Fig. 6: ^1H -NMR-spectra of the ligand **2d** and its copper(I)-complex **6d**.

The ^1H -NMR-spectra of both complexes **6b** and **6d** show symmetrical species, the C_2 -symmetry of the ligand is not broken and therefore the silver(I)-complexes are still C_2 -symmetric (Fig 6b). The broad signals (protons 3', 7 and 9a) in the free ligand (Fig 6a) become sharper upon complexation, indicating that the conformation of the ligand is fixed.

Compared to the published complex **6a**²⁷, only slight changes in the chemical shifts are observed (table 3). In complex **6b**, the signals of the protons 6' and 4' are influenced by the methoxy-phenyl group attached to 5' and show a slight difference of the chemical shift as compared to **6a**.

Table 3 comparison of the chemical shifts of **6a**²⁷ and **6b, d**.

| | 6' | 5' | 4' | 3' | 3 | 4 | 7 | 8 | 9a | 9b | 10 | 12 | 13 | | 6' | 5' |
|----------------------------------|------|------|-------|-------|------|-------|------|-------|-------|------|------|------|------|----------------------------------|------|------|
| 6a ²⁷ | 8.76 | 7.57 | 8.06 | 8.19 | 7.93 | 7.58 | 3.98 | 2.61 | 1.47 | 2.81 | 2.94 | 1.35 | 0.56 | C7 | 8.76 | 7.57 |
| 6b | 8.98 | --- | 8.21 | 8.21 | 7.99 | 7.55 | 4.10 | 2.61 | 1.51 | 2.85 | 2.98 | 1.40 | 0.63 | C8 | 8.98 | --- |
| $\Delta\delta$ | 0.22 | --- | 0.15 | 0.02 | 0.06 | -0.03 | 0.12 | 0.00 | 0.04 | 0.04 | 0.04 | 0.05 | 0.07 | $\Delta\delta$ | 0.22 | --- |
| 6d | --- | 7.79 | 7.95 | 8.16 | 8.15 | 7.52 | 4.08 | 2.6 | 1.46 | 2.81 | 3.01 | 1.39 | 0.65 | C9 | --- | 7.79 |
| $\Delta\delta$ | --- | 0.22 | -0.11 | -0.03 | 0.22 | -0.06 | 0.10 | -0.01 | -0.01 | 0.00 | 0.07 | 0.04 | 0.09 | $\Delta\delta$ | --- | 0.22 |

In complex **6d**, proton 5' nearby the methoxy-phenyl group shows a similar behaviour. Other differences can be explained by the geometry of the complex. The 6'-substituents are pointing towards the metal centre. Therewith they influence strongly the second ligand coordinating to the same centre. This phenomenon has already been observed for the analogous hexanuclear species. Furthermore, the proton signals of the methoxy-phenyl group are shifted to high field ($\Delta\delta = 0.76$ ppm for 8', $\Delta\delta = 0.54$ ppm for 9') as compared to those of the free ligand (also observed in the hexanuclear species, Fig 5b). The electrospray mass spectra of both complexes (**6b** and **6d**) are in accordance with the observations from the NMR-experiments. For both complexes the main peak corresponds to the mononuclear species AgL^+ . The isotopic pattern of these peaks is in excellent agreement to the calculated one (Fig 7).

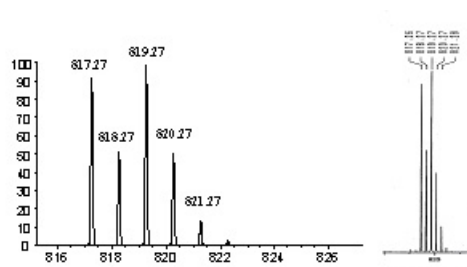


Fig. 7: Calculated (left) and measured (right) isotopic pattern at 819.27 of **6d**.

From the CD-spectra, measured in acetonitrile, the absolute configuration can be attributed to Δ (negative effect of the exciton couplets at 337 nm, Fig 8). While ligand **3b** already shows intense CD-activity assuming a similar structure as in the complex by π - π -stacking, complex **6d** shows a much larger CD-effect than the free ligand **3d**, which implies a conformation change.

Conclusion

Substitution of bridged [5,6]-CHIRAGEN-type ligands with rather large groups does not alter the self assembly behaviour of such molecules significantly.

The same is the case for the directly connected [5,6]-CHIRAGEN[0] derivatives with the respect to their formation of mononuclear complexes.

Experimental part

Complexation reactions

[Ag₆2b₆](PF₆)₆ (4b**)** AgPF₆ (15.5 mg, 0.061 mmol) dissolved in acetonitrile (6 ml) was added to a solution of **2b** (50 mg, 0.061 mmol) in chloroform (2 ml) and acetonitrile (2 ml). This mixture was stirred for 10 minutes at room temperature and the solvent was evaporated under reduced pressure. The white solid (quantitative yield) was used without further purification for the analysis. ¹H-NMR (400 MHz, CD₃CN): δ 8.74 (d, 2H, H(6')), ³J_{6',4'} = 2.0 Hz); 8.29 (d, 2H, H(3)), ³J_{3,4} = 8.3 Hz); 8.24 (d, 4H, H(3')), ³J_{3',4'} = 8.2 Hz); 8.14 (d, 2H, H(4')), ³J_{4',3'} = 8.2 Hz); 7.85 (d, 2H, H(4)), ³J_{4,3} = 8.3 Hz); 7.44 (d, 2H, H(9')),

H(11'), $^3J_{9',8'} = 8.6$ Hz); 6.89 (d, 2H, H(8')), H(12'), $^3J_{8',9'} = 8.6$ Hz); 5.95 (s, 4H, H(3''), H(4''), H(6''), H(7'')); 3.83 (d, 2H, H(1b''), $^2J_{1b'',1a''} = 12.6$ Hz); 3.75 (s, 6H, H(13'')); 2.97 (m, 2H, H(10)); 2.89 (m, 2H, H(7), $^3J_{7,1b''} = 10.5$ Hz); 2.59 (m, 2H, H(9b), $^2J_{9b,9a} = 9.1$ Hz); 2.46 (m, 2H, H(1a'')); 1.60 (d, 2H, H(9a), $^2J_{9a,9b} = 9.1$ Hz); 1.45 (m, 2H, H(8)); 1.22 (s, 6H, H(12)); 0.14 (s, 6H, H(13)). ^{13}C -NMR (100 MHz, CD_3CN): δ 161.5 (Cq); 160.1 (Cq); 151.3 (Cq); 149.1 (Cq); 146.0 (CH, C(6')); 138.4 (Cq); 137.8 (CH, C(4')); 137.4 (CH, C(4)); 137.3 (Cq); 129.2 (CH, C(3'')); 128.9 (CH, C(9'), C(11')); 123.5 (CH, C(3'')); 122.1 (CH, C(3)); 115.6 (CH, C(8'), C(12')); 56.1 (CH_3 , C(13')); 49.6 (CH, C(7)); 47.4 (CH, C(10)); 43.2 (CH, C(8)); 41.6 (Cq, C(11)); 38.5 (CH_2 , C(1'')); 28.2 (CH_2 , C(9)); 26.6 (CH_3 , C(12)); 21.8 (CH_3 , C(13)). ES-MS (CH_3CN): $m/z = 1737.52$ (1+, $[\text{Ag}_2\mathbf{2b}_2]^+$); 1457.96 (4+, $[\text{Ag}_6\mathbf{2b}_6](\text{PF}_6)_2^{4+}$; 2+, $[\text{Ag}_3\mathbf{2b}_3]\text{PF}_6^{2+}$); 1136.53 (5+, $[\text{Ag}_6\mathbf{2b}_6](\text{PF}_6)_2^{5+}$); 922.51 (1+, $[\text{Ag}_2\mathbf{2b}]^+$). UV/Vis: λ_{max} (CH_3CN / nm) 317 ($\epsilon/\text{dm}^3 \text{mol}^{-1} \text{cm}^{-1}$ 7.1×10^4), 273 (2.6×10^4). CD: λ_{max} (CH_3CN / nm) 342 ($\Delta\epsilon/\text{dm}^3 \text{mol}^{-1} \text{cm}^{-1}$ 11.8), 303 (-8.0), 230 (-16.1). Elemental analysis: Found C: 62.4%, H: 4.96, N: 4.58%. $\text{C}_{56}\text{H}_{54}\text{N}_4\text{O}_2\text{AgPF}_6$ requires C: 62.98%, H: 5.10%, N: 5.25%.

$[\text{Cu}_6\mathbf{2b}_6](\text{PF}_6)_6$ (5b) $[\text{Cu}(\text{CH}_3\text{CN})_4]\text{PF}_6^{28}$ (22.8 mg, 0.061 mmol) dissolved in acetonitrile (6 ml) was added to a solution of (50 mg, 0.061 mmol) **2b** in chloroform (2 ml) and acetonitrile (2 ml). Immediately the solution became orange-red. This coloured mixture was stirred for 10 minutes at room temperature and the solvent was evaporated under reduced pressure. The red solid (60.5mg, 97%) was used without further purification for the analysis. ^1H -NMR (400 MHz, CD_3CN): δ 8.48 (d, 2H, H(6'), $^4J_{6',4'} = 2.0$ Hz); 8.33 (d, 2H, H(3'), $^3J_{3',4'} = 8.5$ Hz); 8.32 (d, 4H, H(3), $^3J_{3,4} = 8.1$ Hz); 8.16 (d, 2H, H(4'), $^3J_{4',3'} = 8.5$ Hz, $^4J_{4',3'} = 2.0$ Hz); 7.88 (d, 2H, H(4), $^3J_{4,3} = 8.1$ Hz); 7.40 (d, 2H, H(9'), H(11'), $^3J_{9',8'} = 8.6$ Hz); 6.90 (d, 2H, H(8'), H(12'), $^3J_{8',9'} = 8.6$ Hz); 5.78 (s, 4H, H(3''), H(4''), H(6''), H(7'')); 3.80 (d, 2H, H(1b''), $^2J_{1b'',1a''} = 12.6$ Hz); 3.75 (s, 6H, H(13'')); 3.05 (dd, 2H, H(10), $^3J_{10,9b} = 5.7$ Hz, $^4J_{10,8} = 5.7$ Hz); 2.77 (d, 2H, H(7), $^3J_{7,1b''} = 11.7$ Hz); 2.58 (ddd, 2H, H(9b), $^2J_{9b,9a} = 10.1$ Hz, $^3J_{9b,10} = 5.7$ Hz, $^3J_{9b,8} = 5.7$ Hz); 2.33 (m, 2H, H(1a'')); 1.63 (d, 2H, H(9a), $^2J_{9a,9b} = 10.1$ Hz); 1.40 (m, 2H, H(8)); 1.17 (s, 6H, H(12)); 0.09 (s, 6H, H(13)). ^{13}C -NMR (100 MHz, CD_3CN): δ 160.7 (Cq); 159.0 (Cq); 151.4 (Cq); 150.9 (Cq); 145.9 (CH, C(6')); 138.7 (Cq); 136.6 (CH, C(4')); 135.9 (CH, C(4)); 135.5 (Cq); 128.7

(CH, C(3'')); 128.5 (CH, C(9'), C(11')); 121.8 (CH, C(3')); 120.9 (CH, C(3)); 114.8 (CH, C(8'), C(12')); 55.4 (CH₃, C(13')); 49.0 (CH, C(7)); 46.7 (CH, C(10)); 42.6 (CH, C(8)); 41.8 (Cq, C(11)); 37.3 (CH₂, C(1'')); 27.4 (CH₂, C(9)); 25.8 (CH₃, C(12)); 21.7 (CH₃, C(13)). ES-MS (CH₃CN): m/z = 1693.76 (1+, [Cu $\mathbf{2b_2}$]⁺); 1560.88 (3+, [Cu $\mathbf{52b_5}$](PF₆)₂³⁺); 1390.02 (2+, [Cu $\mathbf{32b_3}$]PF₆²⁺); 1219.79 (2+, [Cu $\mathbf{42b_4}$]PF₆³⁺); 1134.42 (4+, [Cu $\mathbf{52b_5}$]PF₆⁴⁺); 879.35 (1+, 3+, 6+, [Cu $\mathbf{n2b_n}$]ⁿ⁺); 815.43 (1+, [H $\mathbf{2b}$]⁺); 470.15 (2+, [Cu $\mathbf{22b}$]²⁺); 439.18 (2+, [Cu $\mathbf{2b}$]²⁺). UV/Vis: λ_{max} (CH₃CN / nm) 317 (ϵ / dm³ mol⁻¹ cm⁻¹ 6.4*10⁴). CD: λ_{max} (CH₃CN / nm) 345 ($\Delta\epsilon$ / dm³ mol⁻¹ cm⁻¹ 10.1), 282 (-3.6), 242 (3.0), 229 (-10.0).

[Cu $\mathbf{62c_6}$](ClO₄)₆ (**5c**) {6'-Phenyl}-[5,6]-pinene-CHIRAGEN[*p*-xyl] (**2c**) (50 mg, 0.066 mmol) was dissolved in dichloromethane (2 ml) and a solution of Cu(CH₃CN)₄ClO₄²⁹ (22mg, 0.66 mmol) in acetonitrile (2 ml) was added. The colour changed from yellow to deep red. The mixture was stirred for 30 minutes and the solvent was removed under reduced pressure. The red residue was dissolved in acetonitrile and the complex was precipitated adding 5ml of diethylether. The red solid was filtered and dried in vacuum, yielding the complex **5c** (60 mg, 99%). ¹H-NMR (300 MHz, CD₃CN): δ 8.10 (d, 2H, H(3), ³J_{3,4} = 8.1 Hz); 7.91 (d, 2H, H(4), ³J_{4,3} = 8.1 Hz); 7.71 (m, 4H, H(3'), H(4')); 7.35 (dd, 2H, H(5'), ³J_{5',4'} = 7.68 Hz, ³J_{5',3'} = 2.6 Hz); 7.13 (d, 4H, H(8'), H(12'), ³J_{8',9'} = 7.5 Hz); 7.02 (d, 2H, H(10'), ³J_{10',9'} = 7.5 Hz); 6.76 (dd, 4H, H(9'), H(11'), ³J_{9',8'} = 7.5 Hz, ³J_{9',10'} = 7.5 Hz); 5.69 (s, 4H, H(3''), H(4''), H(6''), H(7'')); 4.26 (m, 2H, H(1b'')); 3.12(dd, 2H, H(10), ³J_{10,9b} = 5.5 Hz, ³J_{10,8} = 5.5 Hz); 2.92 (m, 2H, H(7)); 2.66-2.52 (m, 2H, H(9b), H(1a'')); 1.75 (d, 2H, H(9a), ²J_{9a,9b} = 9.9 Hz); 1.45 (m, 2H, H(8)); 1.21 (s, 6H, H(12)); 0.14 (s, 6H, H(13)). ¹³C-NMR (75.4 MHz, CD₃CN): δ 158.6 (Cq); 158.3 (Cq); 153.6 (Cq); 147.0 (Cq); 139.8 (Cq); 139.3 (Cq); 137.0 (CH, C(4')); 136.5 (CH, C(4)); 129.5 (Cq); 129.4 (CH, C(3'')); 128.5 (CH, C(8')); 128.2 (CH, C(10')); 126.3 (CH, C(3')); 122.4 (CH, C(5')); 121.9 (CH, C(3)); 118.2 (CH, C(9')); 48.4 (CH, C10); 47.4 (CH, C7); 43.3 (CH, C8); 41.0 (Cq, C11); 37.3 (CH₂, C1''); 27.9 (CH₂, C9); 26.5 (CH₃, C12); 22.8 (CH₃, C13); ES-MS (CH₃CN): m/z = 1573.55 (1+, [Cu $\mathbf{2c_2}$]⁺); 1430.50 (3+, [Cu $\mathbf{52c_5}$](ClO₄)₂³⁺); 1277.54 (2+, [Cu $\mathbf{32c_3}$]ClO₄²⁺); 1048.03 (4+, [Cu $\mathbf{52c_5}$]ClO₄⁴⁺); 817.38 (1+, 2+, [Cu $\mathbf{n2c_n}$]ⁿ⁺); 755.45 (1+, [H $\mathbf{2c}$]⁺); 441.15 (2+, [Cu $\mathbf{22c}$]²⁺); UV/Vis: λ_{max} (CH₃CN/

nm) 302 ($\epsilon/\text{dm}^3\text{ mol}^{-1}\text{ cm}^{-1}$ 3.92×10^4), 288 (3.21×10^4), 253 (4.8×10^4). CD: λ_{max} ($\text{CH}_3\text{CN}/\text{nm}$) 306 ($\Delta\epsilon/\text{dm}^3\text{ mol}^{-1}\text{ cm}^{-1}$ 6.3), 252 (-6.0), 226 (-21.0).

[Cu₆2d₆](PF₆)₆ (5d) [Cu(CH₃CN)₄]PF₆²⁸ (22.9 mg, 0.061 mmol) dissolved in acetonitrile (6 ml) was added to a solution of **2d** (50 mg, 0.061 mmol) in chloroform (2 ml) and acetonitrile (2 ml). Immediately the solution became orange-red. This coloured mixture was stirred for 10 minutes at room temperature and then about 6 ml of the solvent was evaporated under reduced pressure. The remaining solution was precipitated with diethylether. The precipitate was filtrated over Kieselgur, washed with hexane and chloroform and redissolved in acetonitrile. The solvent was removed under reduced pressure. The orange-red powder was dried in vacuum, yielding the complex **5d** (49 mg, 78%).

¹H-NMR (400 MHz, CD₃CN): δ 8.12 (d, 2H, H(3), ³J_{3,4} = 8.1 Hz); 7.90 (d, 2H, H(4), ³J_{4,3} = 8.1 Hz); 7.68 (m, 4H, H(3'), H(4')); 7.28 (dd, 2H, H(5'), ³J_{5',4'} = 7.3 Hz, ³J_{5',3'} = 2.6 Hz); 7.08 (d, 2H, H(8'), H(12'), ³J_{8',9'} = 8.6 Hz); 6.24 (d, 2H, H(9'), H(11'), ³J_{9',8'} = 8.6 Hz); 5.69 (s, 4H, H(3''), H(4''), H(6''), H(7'')); 4.26 (dd, 2H, H(1b''), ²J_{1b'',1a''} = 12.5 Hz, ³J_{1b'',7} = 3.6 Hz); 3.64 (s, 6H, H(13'')); 3.10 (dd, 2H, H(10), ³J_{10,9b} = 5.6 Hz, ⁴J_{10,8} = 5.6 Hz); 2.93 (m, 2H, H(7), ³J_{7,1b''} = 11.7 Hz); 2.64 (ddd, 2H, H(9b), ²J_{9b,9a} = 10.0 Hz, ³J_{9b,10} = 5.6 Hz, ³J_{9b,8} = 5.6 Hz); 2.56 (m, 2H, H(1a''), J = 12 Hz); 1.77 (d, 2H, H(9a), ²J_{9a,9b} = 10.0 Hz); 1.45 (m, 2H, H(8)); 1.21 (s, 6H, H(12)); 0.14 (s, 6H, H(13))., ES-MS (CH₃CN): m/z = 1691.75 (1+, [Cu₂2d₂]⁺); 1560.55 (3+, [Cu₅2d₅](PF₆)₂³⁺); 1133.43 (4+, [Cu₅2d₅](PF₆)₄⁴⁺); 879.36 (1+, 3+, 6+, [Cu_n2d_n]ⁿ⁺); 815.43 (1+, [H2d]⁺); 470.15 (2+, [Cu₂2d]²⁺); 439.19 (2+, [Cu2d]²⁺). UV/Vis: λ_{max} (CH₃CN / nm) 313 ($\epsilon/\text{dm}^3\text{ mol}^{-1}\text{ cm}^{-1}$ sh, 3.2×10^4), 261 (5.3×10^4), 209 (6.4×10^4), CD: λ_{max} (CH₃CN / nm) 318 ($\Delta\epsilon/\text{dm}^3\text{ mol}^{-1}\text{ cm}^{-1}$ +7.5); 276 (3.0); 258 (-6.3), 226 (-20.9). Elemental analysis: Found C: 63.26%, H: 5.39%, N: 5.14%. C₅₆H₅₄N₄O₂CuPF₆ requires C: 65.71%, H: 5.32%, N: 5.47%.

[Ag3b]PF₆ (6b) Under argon and light protection, AgPF₆ (11.2 mg, 0.045 mmol) dissolved in acetonitrile (6 ml) and added to a solution of **3b** (31.5 mg, 0.045 mmol) in chloroform (6 ml) and actonitrile (4 ml). This mixture was stirred for 30 minutes at room temperature. The solvent was removed under reduced pressure. After drying, a white

solid was obtained (42.5 mg, quantitative yield) and was analysed without further purification.

^1H -NMR (400 MHz, CH_3CN): 8.98 (s, 2H, H(6')); 8.21 (br, 4H, H(3'), H(4')); 7.99 (d, 2H, H(3), $^3J_{3,4} = 7.8$ Hz); 7.55 (br, 4H, H(9'), H(11')); 7.37 (br, 2H, H(4)); 7.03 (d, 4H, H(8'), H(12'), $^3J_{8',9'} = 8.7$ Hz); 4.10 (br, 2H, H(7)); 3.83 (s, 6H, H(13')); 2.98 (m, 2H, H(10)); 2.85 (m, 2H, H(9_b)); 2.61 (m, 2H, H(8)); 1.51 (d, 2H, H(9_a), $^2J_{9a,9b} = 9.8$ Hz); 1.40 (s, 6H, H(12)); 0.63 (s, 6H, H(13)). ^{13}C -NMR (100 MHz, CH_3CN): 161.5 (Cq); 160.7 (Cq); 151.5 (Cq); 150.6 (Cq); 149.2 (CH, C(6')); 145.3 (Cq); 137.3 (Cq); 136.6 (CH, C(4')); 135.2 (CH, C(4)); 133.1 (Cq); 128.7 (CH, C(9'), C(11')); 122.7 (CH, C(3')); 120.1 (CH, C(3)); 115.0 (CH, C(8'), C(12')); 55.4 (CH_3 , C(13')); 47.7 (CH, C(7)); 46.0 (CH, C(10)); 41.8 (Cq, C(11)); 41.4 (CH, C(8)); 31.2 (CH_2 , C(9)); 25.9 (CH_3 , C(12)); 20.6 (CH_3 , C(13)). ES-MS: $m/z = 817.3$ (1+, Ag3b-H^+), 711.3 (1+, $\mathbf{3b}^+$). UV/Vis: λ_{max} (CH_3CN / nm) 321 ($\epsilon/\text{dm}^3 \text{mol}^{-1} \text{cm}^{-1}$ 6.1×10^4), 271 (2.2×10^4 ; sh). CD: λ_{max} (CH_3CN / nm) 337 ($\Delta\epsilon/\text{dm}^3 \text{mol}^{-1} \text{cm}^{-1}$ -100), 302 (47). Elemental analysis: Found C: 59.83%, H: 4.88%, N: 5.45%, $\text{C}_{48}\text{H}_{46}\text{N}_4\text{O}_2\text{AgPF}_6$ requires C: 59.82%, H: 4.81%, N: 5.81%.

[Ag3d]PF₆ (6d) Under argon and light protection, AgPF_6 (17.7 mg, 0.07 mmol) dissolved in acetonitrile (6 ml) was added to a solution of **3d** (50 mg, 0.07 mmol) in chloroform (20 ml) and acetonitrile (5 ml). This mixture was stirred for 3 hours at room temperature. The solvent was removed under reduced pressure. After drying, a white solid was obtained in quantitative yield, and was analysed without further purification.

^1H -NMR (400 MHz, CH_3CN): 8.16 (d, 2H, H(3), $^3J_{3,4} = 7.7$ Hz); 8.15 (d, 2H, H(3'), $^3J_{3',4'} = 7.8$ Hz); 7.95 (dd, 2H, H(4'), $^3J_{4',3'} = 7.8$ Hz, $^3J_{4',5'} = 7.8$ Hz); 7.79 (d, 2H, H(5'), $^3J_{5',4'} = 7.8$ Hz,); 7.52 (d, 2H, H(4), $^3J_{4,4} = 7.7$ Hz); 7.35 (d, 4H, H(8'), H(12'), $^3J_{8',9'} = 8.7$ Hz); 6.47 (br, 4H, H(9'), H(11')); 4.08 (br, 2H, H(7)); 3.61 (s, 6H, H(13')); 3.01 (m, 2H, H(10)); 2.81 (m, 2H, H(9_b)); 2.60 (m, 2H, H(8)); 1.46 (d, 2H, H(9_a), $^2J_{9a,9b} = 9.8$ Hz); 1.39 (s, 6H, H(12)); 0.65 (s, 6H, H(13)). MS(ESI): $m/z = 817.3$ (1+, Ag3d-H^+), 711.3 (1+, $\mathbf{3d}^+$). UV/Vis: λ_{max} (CH_3CN / nm) 318 ($\epsilon/\text{dm}^3 \text{mol}^{-1} \text{cm}^{-1}$ 4.9×10^4), 267 (5.2×10^4 ; sh). CD: λ_{max} (CH_3CN / nm) 337 ($\Delta\epsilon/\text{dm}^3 \text{mol}^{-1} \text{cm}^{-1}$ -67), 292 (21), 224 (-35). Elemental analysis: Found C: 59.3%, H: 4.67%, N: 5.23%; requires: C: 59.82%, H: 4.81%, N: 5.81%

Acknowledgements

This work was supported by Swiss National Science Foundation.

References

- 1 J.-M. Lehn, A. Rigault, J. Siegel, J. Harrowfield, B. Chevrier, D. Moras, *Proc. Natl. Acad. Sci. USA*, 1987, **84**, 2565.
- 2 C. L. Atkin, J. B. Neilands, *Biochemistry*, 1968, **7**, 3734.
- 3 R. C. Scarrow, D. L. White, K. N. Raymond, *J. Am. Chem. Soc.*, 1985, **107**, 6540.
- 4 J. M. Lehn, J. P. Sauvage, J. Simon, R. iessel, C. iccinni-Leopardi, G. Germain, J. P. Declercq, M. Van Meerssche, *Nouv. J. Chim.*, 1983, **7**, 413.
- 5 Van Stein, G. C.; Van der Poel, H.; Van Koten, G.; Spek, A. L.; Duisenberg, A. J. M.; Pregosin, P. S. *J. Chem Soc., Chem. Commun.*, 1980, 1016.
- 6 W. S. Sheldrick, J. Engel, *J. Chem. Soc., Chem. Commun.*, 1980, 5.
- 7 C. J. Carrano, K. N. Raymond, *J. Am. Chem. Soc.*, 1978, **100**, 5371.
- 8 G. Struckmeier, U. Thewalt, J. H. Fuhrhop, *J. Am. Chem. Soc.*, 1976, **98**, 278.
- 9 C. Piguet, G. Bernardinelli, G. Hopfgartner, *Chem. Rev.*, 1997, **97**, 2005.
- 10 M. Albrecht, *Chem. Rev.*, 2001, **101**, 3457.
- 11 G. Baum, E. C. Constable, D. Fenske, C. E. Housecroft, T. Kulke, *J. Chem. Soc., Chem. Comm.*, 1999, 195.
- 12 P. N. W. Baxter, J.-M. Lehn, K. Rissanen, *J. Chem. Soc., Chem. Comm.*, 1997, 1323.
- 13 C. Bonnefous, N. Bellec, R. Thummel, *J. Chem. Soc., Chem. Comm.*, 1999, 1243.

- 14 B. Hasenknopf, J.-M. Lehn, N. Boumediene, A. Dupont-Gervais, A. Van Dorsselaer, B. Kneisel, D. Fenske, *J. Am. Chem. Soc.*, 1997, **119**, 10956.
- 15 C. S. Campos-Fernández, R. Clérac, K. R. Dunbar, *Angew. Chem., Int. Ed.*, 1999, **38**, 3477.
- 16 B. Hasenknopf, J.-M. Lehn, N. Boumediene, E. Leize, A. Van Dorsselaer, *Angew. Chem., Int. Ed.*, 1998, **37**, 3265.
- 17 R. Krämer, J.-M. Lehn, A. De Cian, J. Fischer, *Angew. Chem., Int. Ed.*, 1993, **32**, 703.
- 18 O. Mamula, A. Von Zelewsky, G. Bernardinelli, *Angew. Chem., Int. Ed.*, 1998, **37**, 290.
- 19 T. Bark, M. Duggeli, H. Stoeckli-Evans, A. Von Zelewsky, *Angew. Chem., Int. Ed.*, 2001, **40**, 2848.
- 20 C. Provent, S. Hewage, G. Brand, G. Bernardinelli, L. J. Charbonnière, A. F., *Angew. Chem., Int. Ed.*, 1997, **36**, 1287.
- 21 C. Provent, E. Rivara-Minten, S. Hewage, G. Brunner, A. F. Williams, *Chem. Eur. J.*, 1999, **5**, 3487.
- 22 O. Mamula, F. J. Monlien, A. Porquet, G. Hopfgartner, A. E. Merbach, A. Von Zelewsky, *Chem. Eur. J.*, 2001, **7**, 533.
- 23 M. Duggeli, C. Goujon-Ginglinger, S. Richard Ducotterd, D. Mauron, C. Bonte, A. Von Zelewsky, H. Stoeckli-Evans, A. Neels, *Org. Biomol. Chem.*, 2003, **1**, 1894
- 24 H. Mürner, A. Von Zelewsky, H. Stoeckli-Evans, *Inorg. Chem.* 1996, **35**, 3931
- 25 N. C. Fletcher, F. R. Keene, H. Viebrock, A. Von Zelewsky, *Inorg. Chem.*, 1997, **36**, 1113.
- 26 N. C. Fletcher, F. R. Keene, M. Ziegler, H. Stoeckli-Evans, H. Viebrock, A. Von Zelewsky, *Helv. Chim. Acta*, 1996, **79**, 1192.
- 27 O. Mamula, A. Von Zelewsky, T. Bark, H. Stoeckli-Evans, A. Neels, G. Bernardinelli, *Chem. Eur. J.*, 2000, **6**, 3575.
- 28 G. J. Kubas,, *Inorg. Synth.*, 1979, **19**, 90.
- 29 B. J. Hathaway, D. G. Holah, J. D. Postlethwaite, *J. Chem. Soc.* 1961, 3215.
- 30 O. Mamula, *Thesis No. 1268, University of Fribourg*, 1999.

